Material Science Research India Vol. **11**(1), **27-34** (2014)

Ionic Liquid Controlled Growth of Zinc Oxide Nanoparticles and their Fluorescence study in the presence of NH_3 gas

NEHA SINGH[1], FAZILA SYED[2] and FOZIA Z. HAQUE[1]*

[1]Optical Nanomaterials Lab, Department of Physics,
Maulana Azad National Institute of Technology, Bhopal - 462051, India.
[2]Department of Chemistry, Mumbai University, Mumbai, Maharashtra, India.
*Corresponding author Email: foziazia@rediffmail.com

http://dx.doi.org/10.13005/msri/110104

(Received: August 12, 2014; Accepted: September 02, 2014)

ABSTRACT

This article describes the synthesis of ZnO nanoparticle with an average crystallite size ~20 nm through aqueous solution growth technique using Benzyltrimethylammoium hydroxide Ionic liquid (BTMAH) as a structure directing agent. Crystallinity, phase purity, Volume of unit cell, average crystallite size, and strain were confirmed by X-ray diffraction pattern using Scherrer s method and Williamson-Hall analysis, particle morphology and grain size were confirmed by Atomic force microscopy. Using the optical properties photoluminescence, interaction between ammonia gas and zinc oxide nanoparticle were also investigated. The material shows average significant increment in the PL intensity which conform its tremendous applicability in optical gas sensor to detect ammonia gas (25 ppm).

Key words: ZnO nanoparticles; Ionic liquid; X-ray diffraction; Photoluminescence; Optical gas sensing.

INTRODUCTION

Zinc oxide (ZnO) is a piezoelectric, dielectric and transparent oxide semiconductor, with a direct band gap of 3.37eV at room temperature and a large excitation binding energy (60 meV), which is 2.4 times the effective thermal energy (25meV) at room temperature[1]. As in most II-VI materials, the bonding in ZnO is largely ionic, which explains its strong piezoelectricity. In addition, due to the high melting point (2248 K) and large cohesive energy (1.89 eV), therefore more resistant to wear. Electron mobility in ZnO single crystals is about 200 $cm^2/V.s$ [2,3]. ZnO has several fundamental advantages over its chief competitor GaN, due to its high energy radiation stability and amenability to wet chemical etching. It is highly transparent and has good electrical conductivity that is why it is extensively used for various applications such as gas sensor and photovoltaic devices[4-8]. Ionic liquid have recently emerged as green and environment friendly solvent for their use in the industrial manufacture of chemicals, Ionic liquid are composed of cations and anions having low melting point(< 100°C), while the cations may be organic or anions are inorganic[9-12]. In some cases, ILs and the related IL crystals combine these functions and serve unique system as solvent–reactant–templates, or ionic liquid (crystal) precursors as reported in many studies[13, 14]. The use of ILs in such cases provided easy synthesis of inorganic Nanomaterials and surfaces with novel or improved properties, sometimes resulting into otherwise inaccessible structures with unique properties, and it s also used as a structure directing/ stabilizing agent. The synthesis of ZnO from ionic liquid precursors is mainly concentrated on their crystal growth

aspects. Because of the important application of ZnO as gas sensing materials, the gas sensing properties of synthesized ZnO from the ionic liquid precursor should be highly desired[15].

There are various chemical methods for the synthesis of ultrafine oxide nanoparticles such as sol–gel, hydrothermal, aqueous solution growth technique flame combustion and precipitation[16]. The aqueous solution growth technique is one of the best methods to fabricate material at low cost with mild temperatures, high purity materials with control in the nanostructure and surface properties. The synthesis involves the controlled hetero-nucleation of metal oxides in aqueous solutions[17]. Single-crystal nanostructures can give rise to novel usefull properties in different application fields, such as gas sensing. Indeed, the average surface-to-volume ratio, consequent on the reduced sized of nanostructures leads to an enhanced surface interaction[18]. In particular, sensors based on the variations of the photoluminescence (PL) emission in the presence/absence of gas molecules are attractive because they can provide high responses at room temperature and result stable with a rapid, reproducible and good sensitivity[19]. The prepared material is characterized using powder XRD, SEM, AFM, PL.

EXPERIMENTAL DETAILS

Materials used

All chemicals used in this study were of analytical grade and were used without further purifications. Zinc nitrate hexahydrate [Zn $(NO_3)_2 \cdot 6H_2O$] procured from Merck with 99% purity, was used as the zinc cation precursor, and Benzyltrimethylammoium hydroxide (ionic liquid) (BTMAH) procured from Alpha Aesar as the hydroxide anion precursor. Alkaline solution of NaOH was used to adjust pH.

Aqueous solution growth technique for zinc oxide nanoparticle

ZnO nanoparticles were synthesized by aqueous solution growth technique employing 0.2 M of Zinc Nitrate hexahydrate [Zn $(NO_3)_2 \cdot 6H_2O$] dissolved in 50 ml of double distilled water under magnetic stirring at room temperature. The desired amount of IL was added to above solution, then the required amount of NaOH solution was added to make alkaline concentration (pH 10). The addition of NaOH causes the formation of Zinc hydroxide, which then transforms into ZnO by aqueous solution growth technique. Then prepared solution was kept in a temperature controlled oven at 180°C for 6 h. The white product was separated by centrifugation and washed with double distilled water several times and then dried at 100°C for 2 hrs.

Material characterization

The crystal structure of ZnO powder has been collected in Bruker D8 Advance X-ray powder diffractrometer with CuKα radiation operating at 40 kV and 40 mA. Diffraction peaks of the crystalline phase were compared with those of the standard compounds reported in the JCPDS data files. Scanning Electron Microscope (SEM, JEOL-JSM-6390) and Atomic Force Microscope (NT-MDT Solver NEXT), were used to determine the morphology of IL modified ZnO nanoparticles. The sample was characterized for optical property and gas sensing determination through photoluminescence (PL) spectra at room temperature and the data was recorded using Fluorescence Spectrometer (F-7000 Hitachi) exiting with its xenon lamp at 310 nm for PL.

Gas sensing measurement:

The optical gas sensing measurement was done by exciting by a Xenon light source [F-7000 Hitachi] at 310 nm excitation wavelength at room temperature. To study gas sensing, the sample was placed inside an air tight quartz sample holder and this sample holder was inserted inside the spectrometer chamber for optical measurements. The quartz sample holder is fitted with a suitable inlet and outlet for gases. The data is recorded in the presence of simple air and with 25 ppm ammonia gas.

RESULT AND DISCUSSION

Crystal structure and phase analysis

The structure and phase purity of ionic liquid modified ZnO sample was investigated by powder XRD. The XRD spectra of ZnO nanoparticles are shown in figure 1.The nanoparticles are highly crystalline as can be seen from XRD pattern in which broad peak with high intensity are extended over the 2è.Differection peaks corresponding to reflections peaks of (100), (002), (101), (102), (110), (103), (200), (112), (201), (004), (202) crystal planes respectively, indicative of hexagonal wurtize structures of ZnO [20], which are consistent with standard JCPDS: 792205 card ICSD#: 067454.The

broadening of the diffraction peaks gives an idea about the small particle size and The sharp peaks indicate that the product was well crystallized and oriented of the synthesized ZnO. Crystallite size (D),was calculated by using Debye Scherrer s formula,

$$D=K\lambda/\beta\cos\theta \quad ...(1)$$

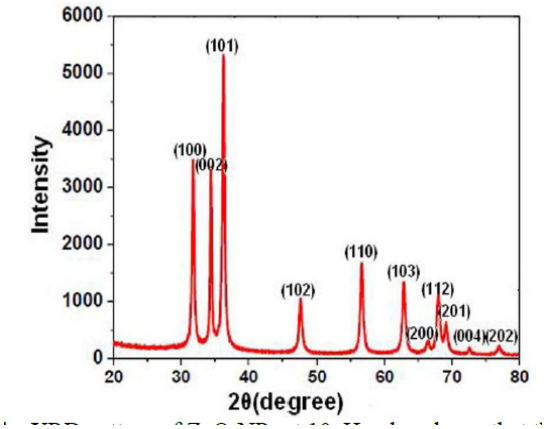

Fig. 1: The XRD pattern of ZnO-NPs at 10pH value shows that the sample product is crystalline with a hexagonal wurtzite phase

Where, K is the particle shape factor which depends on the shape of the particles and its value is 0.94 for spherical particles, λ is CuKα radiations(1.54Å), β is the full width at half maximum (FWHM) of the selected diffraction peaks corresponding to planes, θ is the Bragg angle obtained from 2θ value corresponding to the same plane. The standard XRD pattern of ZnO and their miller indices are used for relative comparison. The results indicate that the product consists of pure phase and there is no impurity reflection peaks.

The calculated crystallite size is presented in Table 1, which are also confirmed by AFM result shown in figure 3. The crystal lattice parameters of powder were heated at 100?C measured by using equation:

$$1/d^2= 4/3\ (h^2+hk+k^2/a^2) + (l^2/c^2) \quad (2)$$

where a and c are the lattice parameters, h, k, and l are the miller indices and d is the interplaner spacing for the plane (hkl). The volume (V) of the unit cell for wurtzite hexagonal system has been calculated using the equation: $V = 1.732.a^2c/ 2 = 0.866\ a^2c$. The variation of lattice parameters and unit cell volume of ZnO nanoparticles is also reported in Table 1.

Williamson-Hall method

The qualitative information of anisotropy in broadening peaks have been determined by using W-H analysis.The W-H method does not follow a 1/ cosè dependency as in the Scherrer equation but instead varies with tanè. The strain induced peak broading in sample due to crystal imperfection and distortion was calculated using the formula:

$$\varepsilon = \beta_{hkl} / 4\tan\theta \quad ...(3)$$

$$\beta_{hkl}\cos\theta = K\lambda/D + 4\varepsilon \sin\theta \quad ...(4)$$

The above equations are W-H equations [21]. For as-prepared ZnO nanoparticles a plot is drawn with βhkl cosθ along the y-axis and 4sinè

Table 1: The lattice parameters, crystalline size, unit cell volume and particle size of ZnO nanoparticles synthesized

Sample treated at 100°C	Lattice Parameters a(Å)	Aspect Ratio (c/a) c(Å)	Volume of unit cell (Å)3	Micro strain	Average crystallite size	Average grain size using AFM (nm) Scherrer s method (nm)	Average particle size using AFM (nm) W-Hmethod (nm)
3.22 20.8	5.26	1.63	47	0.008811	13.61	18.06	11

along the x-axis as shown in Figure 2.

The slope of the curve determines the strain (å) associated with the dislocation and crystallite size. The calculated crystallite sizes and strain is presented in Table 1 using W-H method.

Equation 4 represents the uniform deformation model (UDM), where the strain was assumed to be uniform in all crystallographic directions, thus considering the isotropic nature of the crystal, where the material properties are independent of the direction along which they are measured.

Morphological study of zinc oxide nanoparticles

The surface morphology of the ZnO nanoparticle were examined by Scanning Electron Microscopy (SEM) and Atomic Force Microscope (AFM).The surface morphology of prepared ZnO nanoparticle at desired amount of NaOH and respectively IL concentration. Both NaOH as well as IL has a remarkable effect on the ZnO morphology and particle size. The precipitation reaction is one of the most common liquid phase reactions, which form a solid phase, and has been utilized extensively for the synthesis of large-scale preparation of zinc oxide powders. When an aqueous solution of zinc salts reacts, compounds with low solubility precipitate out of the solutions. The zinc oxide powder can be obtained after centrifugation and drying the precipitates. By employing various salts and controlling processing parameters such as temperature, amount of the salt and the pH value of the solution. This method is especially suited for the large-production of fine particles. In order to understand the effect of pH and IL (BTMAH) on the zinc oxide nanoparticle, we have systematically adjusted the pH value at 10 by using alkali sodium hydroxide solution dilution in the precursor solution as per the microscopic observations (SEM) shown in figure 3(a,b).

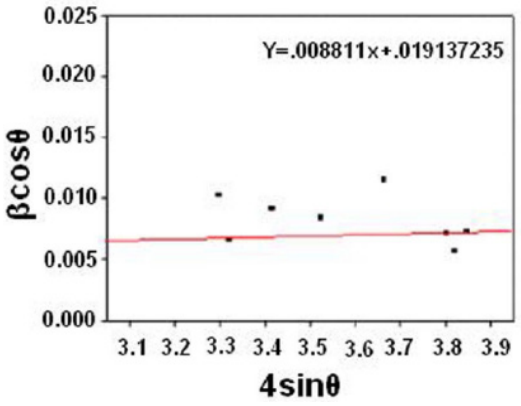

Fig. 2: The W-H analysis of ZnO nanoparticles heated at 100°C assuming UDM. Fit to the data, the strain is extracted from the slope

Compared with SEM, AFM provides extraordinary topographic contrast and unobscured views of surface features. To analyze surface morphology, the 1μm×1μm image was taken from the sample using an Atomic Force Microscope (AFM). Two-dimensional, Three-dimensional image average grain size and average diameter of the sample is shown in figure 4 (a, b, c & d).From this image, it can be seen that dispersion of ZnO nanoparticles is relatively uniform. Average grain size and diameter

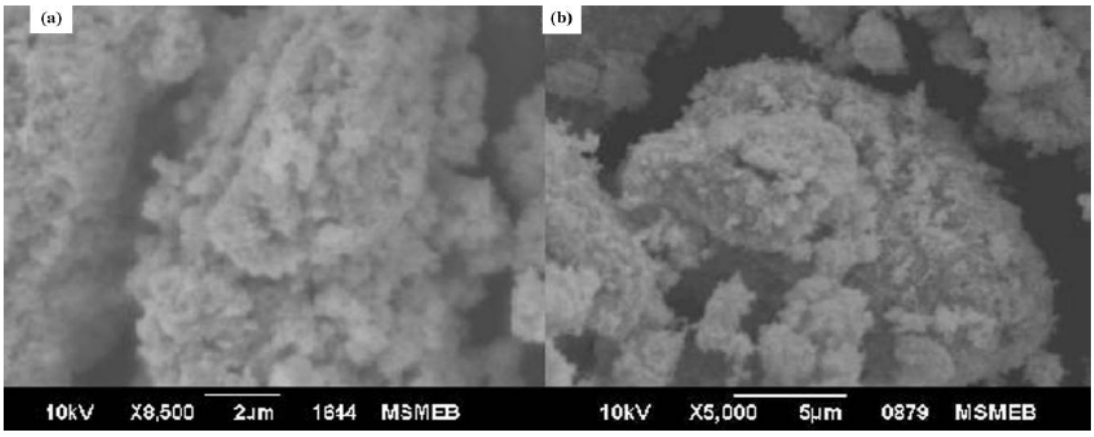

Fig. 3(a,b). SEM images of zinc oxide nanoparticle s with different magnification

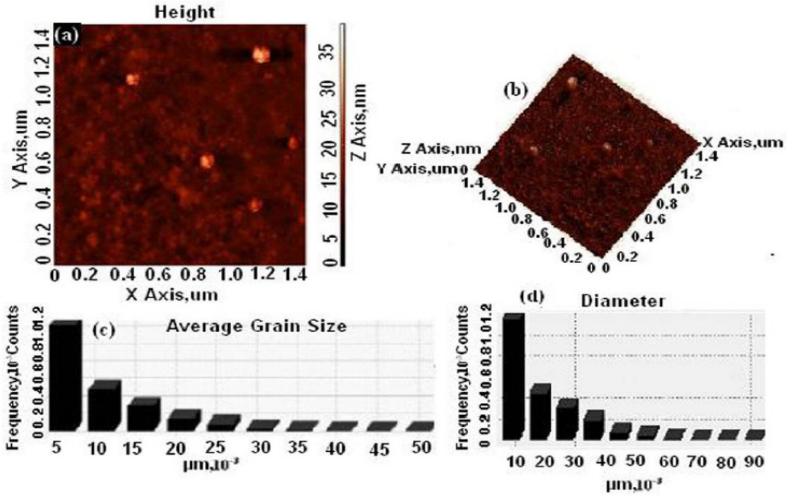

Fig. 4: Atomic Force Microscopic surface morphology analysis of ZnO nanoparticles (a) 2D phase diagram (b) 3D image and (c) Histogram of Average grain size(d)Histogram of Average Diameter of nanoparticles.

of particle were determined with the help of Nova PX analysis software programming. The average grain size of the ZnO sample was found to be 11nm with 20.8nm diameter, and maximum diameter of particle in the sample were found to be 0 to 10nm, which are in good agreement with XRD and SEM results. As seen in AFM images, the ZnO sample was formed from the particles like circles. The particles are well distributed in the sample and the average roughness of sample was estimated ~1.77 nm using Nova PX software.

PL characterization of zinc oxide nanoparticle

Photoluminescence (PL) is the spontaneous emission of light from a material under optical excitation. The excitation energy and intensity are chosen to probe different regions and excitation concentrations in the sample. PL depends on the nature of the optical excitation. The excitation energy selects the initial photo excited state and governs the penetration depth of the incident light. The PL signal often depends on the density of photo excited electrons, and the intensity of the incident beam can be adjusted to control this parameter. When the type or quality of material under investigation varies spatially, the PL signal will change with excitation position[22].

In the photoluminescence spectrum of ZnO nanoparticles synthesized by aqueous solution growth technique at excitation wavelength of 310 nm, in general there are emission bands in the UV and visible regions. The UV peak is usually considered as the characteristic emission of ZnO and attributed to the band edge emission or the exciton transition. In many reports, the characteristic emission of ZnO was absent in their luminescence spectra. Generally the UV emission in ZnO disappears in two cases. First, if the excitation energy is considerably lower that its band gap energy and second, if the intensity of visible emission is much higher due to increased defect density[23].In our case, ultraviolet emission peak not present only visible emission is present as the excitation wavelength is 310nm.

Generally, visible emission in ZnO is due to different intrinsic defect such as oxygen vacancy

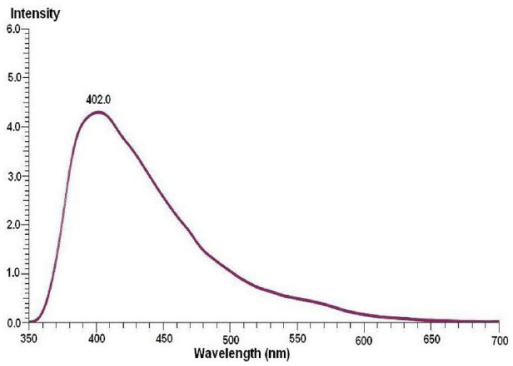

Fig. 5: Room-temperature photoluminescence spectrum ZnO nanoparticle at an excitation wavelength of 310nm

(V_O), zinc vacancy (V_{Zn}), interstitial zinc (Z_{ni}), interstitial oxygen (O_i) and antisite oxygen (O_{Zn}), it is thought that the deep-level emission was caused by different intrinsic defects in ZnO film, such as VO, V_{Zn}, Z_{ni} and O_i. Because the deep-level emission center (2.50 eV) is smaller than the band gap energy of ZnO (3.37 eV), the deep-level emission must be related to the defect level in band gap[23-25].

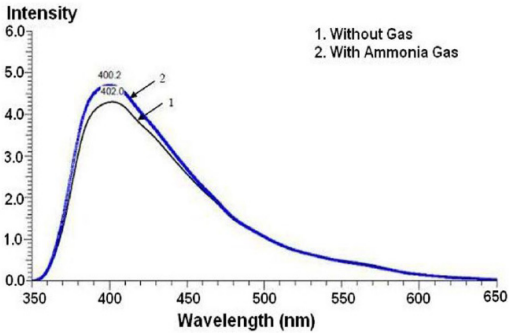

Fig. 6: Shows the overlapped PL spectra of samples taken with and without the exposure of ammonia gas. In both spectra; a strong violet emission and slightly yellow emission also seen.

The PL spectrum of zinc oxide nanoparticle prepared at room temperature shown in figure 5. A strong emission peak was observed around 402.0 (violet emission)3.09eV, which is attributed to the recombination of an electron at the zinc interstitial (Zni) and a hole in the valance band. In ZnO, Zn3d electrons strongly interact with the O_{2p} electron i.e. oxygen has tightly bound 3d electrons, which shows the nuclear attraction efficiently. violet luminescence in spectra at 400.2nm (3.08eV) is attributed to the transition from conduction band to the deep holes trapped levels like interstitial zinc (Zni), and also conform confine particle size and enhanced nucleation in the sample. The yellow emission (slight hump) was observed around 570nm (2.17 eV), which attributed to native defects in ZnO, namely to oxygen interstitials or excess oxygen vacancies in the ZnO is commonly observed in ZnO nanostructures as well. The defect responsible for the yellow emission is not located at the surface and can be eliminated by annealing in hydrogen/argon ambient[26, 27].

In optical gas sensors, the changed PL intensity are related to both physical properties of the analytes such as dipole moment/dielectric constant, and equilibrium concentrations of the analytes inside nanostructured materials [28]. In our case, the enhancement of PL intensity of the ZnO nanoparticles exposed to ammonia gas can be explained by an electron transfer mechanism as follows.

For metal oxide semiconductor-based optical gas sensors, the change in PL intensity is mainly caused by the absorption and desorption of oxygen on the surface of sensing materials. ZnO is an intrinsic n-type semiconductor due to oxygen vacancies and interstitial zinc; with electron are the main carriers. Thus resistance of the ZnO nanoparticles decreases when it is exposed to reducing

gases, such as H_2, CO and NH_3. In case of ZnO sample, Oxygen adsorbed on the surface of ZnO would transform to O- or O_{2-} by capturing electron from the conduction band of ZnO and a depletion layer would form on the surface, which result in a high resistance of ZnO, and low conductivity and low PL intensity. The reaction formula is as follows,

$$O_2+2e- \rightarrow 2O- \quad ...(5)$$

When same sample exposed to ammonia, the adsorbed oxygen ion would react with this reductive gas and release electrons back to the conduction band of ZnO. Which lead to increased carrier concentration, thus reduces the tendency of nonradiative transitions, and consequently results in the PL intensity enhancement. This process could be expressed as follows,

$$2NH_3+3O- \rightarrow 3H_2O+N^{2+}3e- \quad ...(6)$$

A very slight shifting in wavelength is also seen due to change in the value of refractive index. The refractive index of material is changed in presence of ammonia gas (25ppm) which shows variation in band-gap of material.

Figure 6. Room-temperature photoluminescence spectrum of ZnO nanoparticle present/absent of ammonia at an excitation wavelength of 310 nm (a) Blue spectra present of ammonia gas (25 ppm) (b) Black spectra absent of gas.

CONCLUSION

The present work shows that highly hydrated ILs, benzyltrimethylammonium hydroxide BTMAH is an efficient IL for the controlled fabrication of ZnO nanoparticles with spherical shapes. The ZnO nanoparticles were prepared in a controlled manner, through aqueous solution growth technique. These nanoparticles have average crystallite size of 13.61nm, 18.06nm and 11 nm and average particle size or diameter of particle 20.8nm. The violet emission at 400.2nm confirms the oxygen rich condition and attributed to the possible existence of nanoparticle. The optical properties of zinc oxide nanoparticles prepared using IL is systematically investigated in the presence of ammonia gas which confirms its tremendous applicability in optical gas sensors.

ACKNOWLEDGEMENTS

The authors would like to thank UGC-DAE Consortium for Scientific Research INDORE-CENTRE, India for providing XRD facility to characterize materials.

REFERENCES

1. Nakahara K., Takasu H., Interactions between gallium and nitrogen dopants in ZnO films grown by radical-source molecular-beam epitaxy, *Appl. Phys. Lett.,* **25**(79): 4139-4141 (2001).
2. Huston A. R., Hall effect studies of doped zinc oxide single crystals, *Phys. Rev.*, **2** (108): 222-230 (1957) .
3 Norton D. P., Ivill, M., Li Y., Kwon Y. W., Erie J. M., Kim H. S., Ip K., Pearton S. J., Heo Y. W., Kim S., Kang B. S., Ren F., Hebard A. F., Kelly J, Charge carrier and spin doping in ZnO thin films, Thin Solids Films, **496**: 160-168 (2006).
4. Martin R., Fortunato Nunes P., Ferreira I., Marques A., Bender M., Katsarakis N., Cimalla V., Kiriakidis G., Zinc oxide as an ozone sensor, *J. Appl. Phys.*, **3**(96) 1398-1407 (2004) .
5. Rao B. B., Zinc oxide ceramic semi-conductor gas sensor for ethanol vapour, *Mater. Chem. Phys.*, **64**: 62-65 (2000).
6. Fortunato E., Goncalves A., Marques A., Viana A., Aguas H., Pereira L., Ferreira I., Vilarinho P., Martins R., New developments in gallium doped zinc oxide deposited on polymeric substrates by RF magnetron sputtering", *Surf. Coat. Technol.,* (180-181), 20-25 (2004).
7. Singh N., Mehra R. M., Kapoor A, Synthesis and characterization of ZnO nanoparticles, *J. Nano-Electron Phys.,* **3**(1): 132-139 (2011).
8. Kumar V., Singh R.G., Purohit L., Mehra R.M., Structural, transport and optical properties of boron doped zinc oxide nanocrystalline, *J. Mater. Sci. Technol.,* **27**(6): 481-488 (2011).
9. Nageshewar d Khupse & Anil Kumar, Ionic liquid: New materials with wide applications, *Indian journal of chemistry*, **49A**: 635-648 (2010).
10. Wasserscheid P., Welton T., (eds) , Ionic Liquids in Synthesis, Wiley New York NY, (2003).
11. Rogers R. D., Seddon K. R., Chemistry. Ionic liquids–solvents of the future?, Science (New York, N.Y.), **302**: 792-793 (2003).
12. Seddon K. R., Ionic liquids: a taste of the future, Nature Mat., 2 (2003) 363–365.
13. Taubert A., Arbell I., Mecke A., Graf P., Photoreduction of a crystalline Au(III) complex: A solid-state approach to metallic nanostructures, *Gold Bull.,* **39**: 205-211 (2006) .
14. Zhu H., Huang J-F., Pan Z., Dai S., Ionothermal synthesis of hierarchical ZnO nanostructures from ionic-liquid precursor, *Chem. Mater.,* **18**: 4473–4477 (2006).
15. Tejwant Singh, Tushar J. Trivedi, Arvind Kumar, Ionic liquid-assisted preparation of ZnO nanostructures, Nanomaterials and Energy , **1**(NME4) (21/05/2012), Pages 207–215.
16. P. Chand, A. Gaur, A. Kumar, Structural and optical properties of ZnO nanoparticles synthesized at different pH values, *J. Alloys Comp.*, **539**: 174–178 (2012).
17. F. Z. Haque, N. Singh, P. Pandey, M. R. Parra, Study of Zinc Oxide nano/micro rods

grown on ITO and glass substrates, Optik - International Journal for Light and Electron Optics, Available online 8 March 2013.

18. C. Baratto , S. Todros ,G. Faglia ,E. Comini ,G. Sberveglieri , S. Lettieri , L. Santamaria ,P. Maddalena, Luminescence response of ZnO nanowires to gas adsorption, Sensors and Actuators B: Chemical, **140**(2): 461–466 (2009).
19. D. Valerini , A. Cretì ,A.P. Caricato ,M. Lomascolo , R. Rella ,M. Martino, Optical gas sensing through nanostructured ZnO films with different morphologies, Sensors and Actuators B: Chemical, **145**(1): 167–173 (2010).
20. Esmaielzadeh kandjani, A.; Shokuhfar, A.; Farzalipour Tabriza, M.; Arefiana, N.A.; Vaezia, M.R., Optical properties of sol-gel prepared nano ZnO. The effects of aging period and synthesis temperature, J. Optoelectron: *Adv. Mater.*, **3**(11): 289-295 (2009).
21. A. Khorsand Zak , W.H. Abd. Majid ,M.E. Abrishami ,Ramin Yousefi, X-ray analysis of ZnO nanoparticles by Williamson–Hall and size–strain plot methods, *Solid State Sciences,* **13**(1): 251–256 (2011).
22. Saroj Kumar Patra, a novel chemical approach to fabricate ZnO nanostructures, master of technology(thesis).
23. Padmini Pandey, Neha Singh, Fozia Z. Haque, Development and optical study of hexagonal multi-linked ZnO micro-rods grown using hexamine as capping agent, *Optik,* **124**(12): 1188–1191 (2013).
24. S.K.Gupta,Aditee Joshi and Manmeet Kaur, Development of gas sensors using ZnO nanostructures, *J.Chem. Sci.,* **122**(1): 57-62 (2010).
25 Tapas Kumar Kundu, Nantu Karak, Puspendu Barik, Satyajit Saha, Optical properties of ZnO nanoparticles prepared by chemical method using poly (vinylalcohol) (PVA) as capping agent, *Int. J. Soft Comp. Eng.,* **1**: 19-24 (2011).
26. Liu M., Kitai A.H., Mascher P, Point defects and luminescence centers in zinc oxide and zinc oxide doped with manganese *J. Lumin.* **54**: 35–42 (1992).
27. Wu X.L., Siu G.G., Fu C.L., Ong H.C, " Photoluminescence and cathodolumine scence studies of stochiometric and oxygen deficiency in ZnO" *Appl. Phys. Lett.*, **78**: 2285–2287 (2001).
28. Jun Xu, Weixin Zhang, Zeheng Yang, Shaixia Ding, Chunyan Zeng, Lingling Chen, Qiang Wang, and Shihe Yang, Large-Scale Synthesis of Long Crystalline Cu2-xSeNanowire Bundles by Water-Evaporation-Induced SelfAssembly and Their Application in Gas Sensing, *Adv. Funct. Mater.*, **19**: 1759–1766 (2009).